

# Sparse Bounded Degree Sum of Squares Optimization for Certifiably Globally Optimal Rotation Averaging

Matthew Giamou\*, Filip Maric, Valentin Peretroukhin, Jonathan Kelly  
University of Toronto

## Abstract

Estimating unknown rotations from noisy measurements is an important step in SfM and other 3D vision tasks. Typically, local optimization methods susceptible to returning suboptimal local minima are used to solve the rotation averaging problem. A new wave of approaches that leverage convex relaxations have provided the first formal guarantees of global optimality for state estimation techniques involving  $SO(3)$ . However, most of these guarantees are only applicable when the measurement error introduced by noise is within a certain bound that depends on the problem instance’s structure. In this paper, we cast rotation averaging as a polynomial optimization problem over unit quaternions to produce the first rotation averaging method that is formally guaranteed to provide a certifiably globally optimal solution for any problem instance. This is achieved by formulating and solving a sparse convex sum of squares (SOS) relaxation of the problem. We provide an open source implementation of our algorithm and experiments, demonstrating the benefits of our globally optimal approach.

## 1. Introduction

Estimating orientations is the principal challenge for many important 3D vision systems. For example, in order to autonomously perform useful tasks, mobile robots need to safely navigate their environment. When a map is unavailable, structure from motion (SfM) or simultaneous localization and mapping (SLAM) is used to build a map while keeping track of a robot’s trajectory. The nonlinear and non-convex constraints of  $SE(3)$  and  $SO(3)$  variables make solving 3D state estimation problems extremely difficult, and a variety of approaches have been proposed over the past few decades. A combination of probabilistic graphical modelling and local optimization methods has steadily become the *de facto* gold standard approach to solving large-scale 3D SLAM problems [4], but these methods often fail with-

\*The corresponding author can be reached at matthew.giamou@robotics.utias.utoronto.ca.

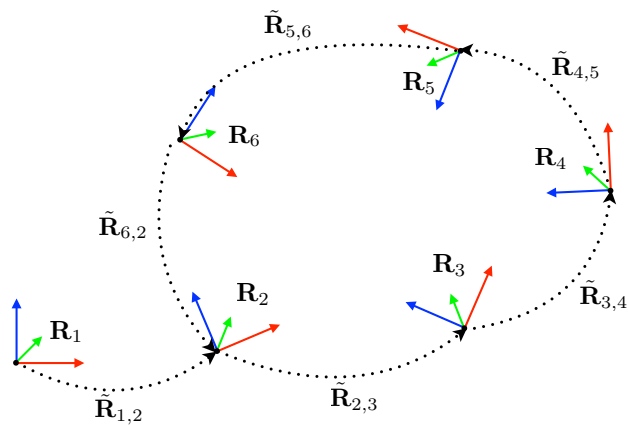


Figure 1: Multiple rotation averaging involves estimating absolute orientations  $\mathbf{R}_i \in SO(3)$  given noisy pairwise relative measurements  $\tilde{\mathbf{R}}_{i,j} \in SO(3)$  recovered by cameras or other sensors.

out a good initialization or in the presence of severe noise. However, recent advances in optimization theory have led to *globally optimal* methods that use convex relaxations of state estimation problems [22, 2, 18, 8, 26]. This strategy has led to fast solvers that return solutions that can be *certified* as globally minimal by comparing the gap between the original and relaxed problems’ cost functions’ values at the candidate solution.

In many camera-based applications, uncoupling position is a practical strategy, or position is either unobservable or known [6]. This leads to the  $SO(3)$  synchronization or “rotation averaging” problem, which retains the difficult non-convex constraints that make full 3D pose estimation challenging. The *multiple* rotation averaging problem (henceforth simply referred to as rotation averaging) involves solving for a number of absolute orientations related by noisy relative measurements (see Figure 1). A thorough survey of the rotation averaging problem is given in [11], wherein two related variants of the problem (single and conjugate rotation averaging) are also examined.

## 1.1. Contributions

In this work, we examine rotation averaging through the lens of recent sum of squares (SOS) polynomial optimization research. Our approach is inspired by the algorithm in [18] for 2D SLAM problems, which makes use of the sparse bounded degree SOS (Sparse-BSOS) optimization method presented in [27]. Our main contributions are:

1. a discussion and comparison of polynomial optimization formulations of rotation averaging;
2. a formal proof that our method is the first multiple rotation averaging solver that is certifiably globally optimal for all problem instances;
3. and an open source implementation of our algorithm and experiments using the Sparse-BSOS Matlab package<sup>1</sup>.

Formal performance guarantees are essential for autonomous vehicles and other safety-critical applications of computer vision. Our hope is that this first application of SOS optimization to a challenging rotation estimation problem will motivate further development of this powerful family of techniques for estimation problems in vision and robotics. Moreover, the novel global optimality guarantees of our approach shed new light on the structure of difficult 3D rotation optimization problems, adding to a growing body of theoretical results in this domain (see, e.g., [28, 8, 9, 26]).

## 1.2. Related Work

Globally optimal solutions to 3D vision and state estimation problems were considered in [19] via convex Lagrangian duality-based relaxations. More recently, Lagrangian duality has been applied to SLAM [5, 22, 2], relative camera pose estimation [3], sensor calibration [10], and rotation averaging problems [8]. These approaches provide fast solution and verification methods for 3D optimization, but only when measurement error is bounded by a problem instance-specific value that is often not straightforward to compute. Furthermore, for most duality-based approaches there do not yet exist formal proofs of global optimality and certification is done on a post-hoc, per-problem instance basis.

Sum of squares (SOS) optimization is a set of approaches that uses theoretical results in real algebraic geometry to solve feasibility and optimization problems with polynomial variables and constraints [20, 14]. These techniques have been applied to numerous problems in probability, statistics, control theory, and finance for almost two decades but have only recently found limited application to state

estimation problems in computer vision and robotics [15]. For example, SOS optimization is used in [12] to find globally optimal solutions to hand-eye and robot-world calibration problems. It was also applied to the *single* and *conjugate* rotation averaging problems in [13]. These problems are noteworthy because they are focused on estimating a small, fixed number of variables representing extrinsic calibration parameters, making them amenable to SOS techniques which typically scale poorly with the number of variables and constraints. Our work is similar to these approaches but uses sparsity properties and a newer SOS relaxation hierarchy to provide faster performance with formal optimality guarantees on the more challenging multiple rotation averaging problem.

More recently, a solution to 2D SLAM (with and without landmarks) that is guaranteed to *always* be globally optimal, regardless of the magnitude of errors present in measurements, was developed in [18]. A new SOS relaxation hierarchy called Sparse Bounded Degree Sum of Squares (Sparse-BSOS) [27] was applied to a polynomial optimization formulation of 2D SLAM to provide strong theoretical guarantees. Although the runtime is too slow for real-time applications, the algorithm in [18] is an important step towards using SOS techniques in practical, large-scale robotic state estimation problems. In this paper, we parallel the approach of [18] to develop the same guarantees for 3D rotation averaging. In particular, we leverage properties of unit quaternion-based rotation averaging to present a method with provable optimality guarantees.

## 2. Problem Formulation

This section describes notation and the rotation averaging problem formulation used throughout the paper. Quaternionic and chordal cost functions are briefly compared. Polynomial representations of SO(3) constraints are developed to conform with the structure required by Sparse-BSOS in Section 3.1.

### 2.1. Notation

Boldface is used for vector and matrix variables with lowercase and uppercase letters respectively (e.g.,  $\mathbf{x}$ ,  $\mathbf{A}$ ). The identity matrix is written  $\mathbf{I}_{n \times n}$ , and the matrix of zeros of size  $m \times n$  is denoted  $\mathbf{0}_{m \times n}$  (or without subscripts when the dimensions can be easily inferred from context). The  $p$ -norm of a vector  $\mathbf{x}$  is denoted  $\|\mathbf{x}\|_p$ , with the Euclidean or 2-norm implied when  $p$  is omitted. The Frobenius norm of a matrix is denoted  $\|\mathbf{A}\|_F$ . We use  $[n]$  as shorthand for the set  $\{1, \dots, n\}$ . The ring of polynomials in the  $n$  scalar variables  $x_i$  of  $\mathbf{x} \in \mathbb{R}^n$  is denoted  $\mathbb{R}[\mathbf{x}]$ . The ring of polynomials only involving some subset of the variables in  $\mathbf{x}$  indexed by  $I \subseteq [n]$  is denoted  $\mathbb{R}[\mathbf{x}; I]$ .

We make extensive use of unit quaternions to represent absolute orientations and relative orientation measurements.

<sup>1</sup> <https://github.com/utiasSTARS/sos-rotation-averaging>

The vector

$$\mathbf{q} = [q_w \ q_x \ q_y \ q_z]^T \in \mathbb{R}^4 \quad (1)$$

is used to represent the quaternion

$$q = q_w + q_x \mathbf{i} + q_y \mathbf{j} + q_z \mathbf{k} \in \mathbb{H}. \quad (2)$$

We write a quaternion representing the  $i$ th absolute orientation in an ordered set as  $\mathbf{q}_i$  and write the relative pose between orientations  $i$  and  $j$  as  $\mathbf{q}_{i,j}$  such that

$$\mathbf{q}_j = \mathbf{q}_i \circ \mathbf{q}_{i,j}, \quad (3)$$

where  $\circ$  represents standard quaternion multiplication. Measurements of relative poses are denoted  $\tilde{\mathbf{q}}_{i,j}$ . Note that unit quaternions constitute a “double cover” of  $\text{SO}(3)$  in that  $\mathbf{q}_i$  and  $-\mathbf{q}_i$  represent the same rotation. Because of this, the quaternion distance metric describing how close two quaternions  $\mathbf{q}_i$  and  $\mathbf{q}_j$  are in the ambient Euclidean space is [11]:

$$\min(\|\mathbf{q}_i - \mathbf{q}_j\|, \|\mathbf{q}_i + \mathbf{q}_j\|). \quad (4)$$

## 2.2. Rotation Averaging

Rotation averaging refers (among other closely related definitions) to the problem of determining a set of absolute orientations (i.e.,  $\text{SO}(2)$  or  $\text{SO}(3)$  elements) given a set of noisy relative orientation measurements (also represented by  $\text{SO}(2)$  or  $\text{SO}(3)$  elements). An instance of the rotation averaging problem consists of a set of relative orientation measurements  $\{\tilde{\mathbf{R}}_{i,j}\}$ ,  $(i,j) \in \mathcal{E}$  where  $\mathcal{E}$  is a set of  $M$  directed edges in the graph relating absolute orientation variables  $\mathbf{R}_i$ ,  $i = 1, \dots, N$ . We can derive a maximum likelihood estimate (MLE) if we assume each noisy measurement  $\tilde{\mathbf{R}}_{i,j}$  is generated by a Langevins distribution [5] with concentration parameter  $\omega_{i,j}^2$ :

$$\tilde{\mathbf{R}}_{i,j} = \mathbf{R}_i^T \mathbf{R}_j \mathbf{R}_\epsilon, \quad (5)$$

$$\mathbf{R}_\epsilon \sim \text{Langevins}(\mathbf{I}, \omega_{i,j}^2). \quad (6)$$

The MLE for this problem can be written as a minimization of the sum of the negative log-likelihoods of each independent measurement:

$$f^* = \underset{\mathbf{R}_i \in \text{SO}(3)}{\text{minimize}} \sum_{(i,j) \in \mathcal{E}} -\log \mathcal{L}(\tilde{\mathbf{R}}_{i,j} | \mathbf{R}_i, \mathbf{R}_j). \quad (7)$$

The log-likelihood of a Langevins distributed error is analogous to that of the Gaussian distribution for linear systems in that it has the following desirable least-squares form:

$$-\log \mathcal{L}(\tilde{\mathbf{R}}_{i,j} | \mathbf{R}_i, \mathbf{R}_j) = \frac{\omega_{i,j}^2}{2} \|\mathbf{R}_i \tilde{\mathbf{R}}_{i,j} - \mathbf{R}_j\|_F^2, \quad (8)$$

which makes this formulation of rotation averaging a quadratically constrained quadratic program (QCQP) when the design variables used are the full rotation matrices  $\mathbf{R}_i \in$

$\mathbb{R}^{3 \times 3}$ . The norms in the cost function are also known as *chordal* distances [11], and they are related to the angular or *geodesic* distances  $\theta = \|\log(\mathbf{R}_a^T \mathbf{R}_b)\|$  as follows:

$$\|\mathbf{R}_a - \mathbf{R}_b\|_F = 2\sqrt{2} \sin(\theta/2). \quad (9)$$

Similarly, the quaternion distance is related to  $\theta$  via:

$$\min(\|\mathbf{q}_a - \mathbf{q}_b\|, \|\mathbf{q}_a + \mathbf{q}_b\|) = 2 \sin(\theta/4). \quad (10)$$

As we will demonstrate in Section 3.1, we are interested in polynomial cost functions and constraints, which the chordal or MLE formulation of 7 has been shown to exhibit ( $\text{SO}(3)$  constraints can be written as quadratic equations). In order to make the quaternion distance quadratic, we can fix the “sign”  $\epsilon_{i,j} \in \{-1, 1\}$  of all measurement quaternions  $\tilde{\mathbf{q}}_{i,j}$  to get the following QCQP:

$$\begin{aligned} & \underset{\mathbf{q}_i}{\text{minimize}} \sum_{(i,j) \in \mathcal{E}} \|\mathbf{q}_i \circ (\epsilon_{i,j} \tilde{\mathbf{q}}_{i,j}) - \mathbf{q}_j\|^2, \\ & \text{s.t.} \quad \mathbf{q}_i^T \mathbf{q}_i = 1, \quad i = 1, \dots, N. \end{aligned} \quad (11)$$

Note that with  $M$  measurements, there are  $2^M$  distinct cost functions possible. In Section 4.1 we describe the method we use to make a favourable selection of quaternion signs  $\epsilon_{i,j}$ .

We can also write the cost function of 11 as

$$f = \sum_{(i,j) \in \mathcal{E}} f_{i,j}, \quad (12)$$

where each term is

$$\begin{aligned} f_{i,j} &= \|\mathbf{Q}_{i,j} \mathbf{q}_i - \mathbf{q}_j\|^2, \\ &= \|\mathbf{Q}_{i,j} - \mathbf{I}\| [\mathbf{q}_i^T \ \mathbf{q}_j^T]^T \|^2, \\ &= [\mathbf{q}_i^T \ \mathbf{q}_j^T] \mathbf{A} [\mathbf{q}_i^T \ \mathbf{q}_j^T]^T, \end{aligned} \quad (13)$$

where

$$\begin{aligned} \mathbf{A} &= [\mathbf{Q}_{i,j} - \mathbf{I}]^T [\mathbf{Q}_{i,j} - \mathbf{I}], \\ &= \begin{bmatrix} \mathbf{I} & -\mathbf{Q}_{i,j} \\ -\mathbf{Q}_{i,j} & \mathbf{I} \end{bmatrix}, \end{aligned} \quad (14)$$

and

$$\mathbf{Q}_{i,j} = \epsilon_{i,j} \begin{bmatrix} q_{w,i,j} & -q_{x,i,j} & -q_{y,i,j} & -q_{z,i,j} \\ q_{x,i,j} & q_{w,i,j} & q_{z,i,j} & -q_{y,i,j} \\ q_{y,i,j} & -q_{z,i,j} & q_{w,i,j} & q_{x,i,j} \\ q_{z,i,j} & q_{y,i,j} & -q_{x,i,j} & q_{w,i,j} \end{bmatrix}, \quad (15)$$

is the right multiplication matrix composed of elements of  $\tilde{\mathbf{q}}_{i,j}$  such that  $\mathbf{Q}_{i,j} \mathbf{q}_i = \mathbf{q}_i \circ \tilde{\mathbf{q}}_{i,j}$ . For the sake of the proof of Theorem 1 in Section 3.3, note that the unit norm equality constraint of a quaternion can be rewritten as the following equivalent inequalities:

$$\begin{aligned} 0 &\leq 1 - \mathbf{q}_i^T \mathbf{q}_i \leq 1, \\ 0 &\leq 2 - \mathbf{q}_i^T \mathbf{q}_i \leq 1. \end{aligned} \quad (16)$$

This simple way of writing our equality constraint with 4 inequality constraints (2 of which are redundant) will be used by the Sparse-BSOS algorithm in Section 3.1. We can now write Problem 11 in the following form:

$$\begin{aligned} & \underset{\mathbf{q}_i}{\text{minimize}} \quad f, \\ & \text{s.t.} \quad 0 \leq g_j \leq 1 \quad \forall j \in [M], \end{aligned} \quad (17)$$

where the  $M = 2N$  constraints capture the unit norm of each unit quaternion variable. Finally, note that there are infinite solutions to Problem 17 due to the gauge symmetry of the problem: for any solution  $\{\mathbf{q}_i\}_{i \in [N]}$  and any unit quaternion  $\mathbf{q}$ , we can apply  $\mathbf{q} \circ \mathbf{q}_i$  to all  $\mathbf{q}_i$  to obtain another solution that is also a minimizer of Problem 17. We resolve this issue by adding constraints that ‘anchor’ the first variable as  $\mathbf{q}_1 = [1 \ 0 \ 0 \ 0]^T$ .

### 3. Sum of Squares Optimization

In this section, we briefly review sum of squares (SOS) optimization and present the Sparse-BSOS hierarchy used by our rotation averaging algorithm. We then prove that our algorithm globally optimally solves any instance of Problem 17. This guarantee is contrasted with the rotation averaging formulation that uses chordal loss and full rotation matrices.

#### 3.1. SOS Optimization

Sum of squares (SOS) optimization is an approach for solving polynomial optimization problems. Techniques in the SOS literature leverage results from real algebraic geometry to provide certificates of feasibility for polynomial inequalities. Various SOS-based techniques have been applied to problems in control theory and many branches of engineering since the early 2000s, but they remain underutilized in the state estimation literature. One reason for this lack of popularity is slow runtime that does not scale well as the number of optimization variables increases. This is a problem for applications like SfM where the number of variables and constraints grow rapidly with the number of measurements available. In this work, we utilize the recent Sparse-BSOS hierarchy of [27] because it is designed with sparse problems like rotation averaging in mind. The interested reader can examine [20] and [15] for in-depth introductions to SOS optimization. The Sparse-BSOS method of [27] is a sparse extension of [17], which introduced a SOS hierarchy with finite convergence guarantees (i.e., globally optimal solutions will *always* be obtained when certain conditions in the problem setup are met).

#### 3.2. Sparse-BSOS

For a complete treatment of the Sparse-BSOS hierarchy, please refer to [27] and [18]. Briefly, we are interested in solving the optimization problem

$$t^* = \sup_{t \in \mathbb{R}} \{t | f(\mathbf{x}) - t \geq 0, \forall \mathbf{x} \in \mathbf{K}\}, \quad (18)$$

where  $\mathbf{K} = \{\mathbf{x} \in \mathbb{R}^n | 0 \leq g_j(\mathbf{x}) \leq 1, j = 1, \dots, m\}$  is the semialgebraic set defined by our constraints. This is equivalent to solving Problem 17. The key insight of SOS optimization is that this problem (and other polynomial optimization problems) can be solved as a semidefinite program (SDP) with Positivstellensatz results from real algebra [15, 20]. Many SOS relaxation hierarchies have been developed, but we use the sparse bounded-degree SOS (Sparse-BSOS) hierarchy of [27] because it leverages the sparsity of rotation averaging, and provides theoretical guarantees for our particular formulation. The method enforces  $f(\mathbf{x}) - t \geq 0$  by introducing the function

$$\begin{aligned} h_d(\mathbf{x}, \boldsymbol{\lambda}) &= \sum_{\alpha, \beta \in \mathbb{N}^m}^{\|\alpha\|_1 + \|\beta\|_1 \leq d} \lambda_{\alpha\beta} h_{d, \alpha\beta}(\mathbf{x}), \\ h_{d, \alpha\beta}(\mathbf{x}) &:= \prod_{j=1}^m g_j(\mathbf{x})^{\alpha_j} (1 - g_j(\mathbf{x}))^{\beta_j}, \quad \mathbf{x} \in \mathbb{R}^n, \end{aligned} \quad (19)$$

where  $\boldsymbol{\lambda}$  contains the coefficients  $\lambda_{\alpha\beta} \geq 0$  indexed by  $\alpha$  and  $\beta$ , and the parameter  $d$  allows us to restrict the number of monomials used to construct  $h_d$ . Now we seek to optimize

$$t^* = \sup_{t, \boldsymbol{\lambda}} \{t | f(\mathbf{x}) - t - h_d(\mathbf{x}, \boldsymbol{\lambda}) \geq 0, \forall \mathbf{x}, \boldsymbol{\lambda} \geq 0\}, \quad (20)$$

where  $h_d(\mathbf{x}, \boldsymbol{\lambda}) > 0$  when  $\mathbf{x} \in \mathbf{K}$  (see [17] for details). Next, the problem is converted to an SDP by restricting the search to  $\Sigma[\mathbf{x}]_k$ , the set of SOS polynomials of degree at most  $2k$ , which constitute a subset of nonnegative polynomials:

$$q_d^k = \sup_{t, \boldsymbol{\lambda}} \{t | f(\mathbf{x}) - t - h_d(\mathbf{x}, \boldsymbol{\lambda}) \in \Sigma[\mathbf{x}]_k, \forall \mathbf{x}, \boldsymbol{\lambda} \geq 0\}. \quad (21)$$

Each  $q_d^k$  describes a level of the BSOS hierarchy indexed by  $d$  and  $k$  [17]. Finally, to produce the Sparse-BSOS hierarchy we partition Problem 21 into smaller blocks of variables and relevant constraints. These subsets of variables, which we denote  $I_l \subseteq [n], \forall l \in [p]$ , must satisfy a sparsity property called the running intersection property (RIP) described in Section 4.2.

#### 3.3. Exactness of Sparse-BSOS

In this section, we prove that using Sparse-BSOS produces an algorithm that *always* returns the global optimum for rotation averaging. In [18], the sparse bounded sum of squares (Sparse-BSOS) hierarchy [27] was used to solve planar pose graph and landmark SLAM. Furthermore, a proof that the first relaxation (corresponding to  $d = 1, k = 1$ ) in the Sparse-BSOS hierarchy will *always* produce the global optimum was provided. In this section, we prove the same result for Problem 17.

**Theorem 1.** *If the running intersection property (RIP) holds for the cost function  $f$  and a variable partition  $\{I_l\}, l = 1, \dots, p$  of an instance of Problem 17, then that instance is solved exactly by the Sparse-BSOS optimization problem when  $k = 1$  and  $d = 1$  (i.e., at the first level of the hierarchy).*

*Proof.* According to Theorem 3 in [27], since each quaternion's constraints are a compact set, it suffices to show that:

1.  $f$  is SOS-convex;
2. each  $-g_j$  is SOS-convex;
3. and for all  $l \in [p]$ , the constraints  $(g_j)_{j \in J_l}$  along with 1 can generate  $\mathbb{R}[\mathbf{x}; I_l]$  as a quadratic module, where  $J_l$  indexes the constraints relevant to the variables indexed by  $I_l$  (see Section 4.2).

A function  $h$  is SOS-convex if its Hessian  $\nabla^2 h$  can be written  $\nabla^2 h = \mathbf{L}\mathbf{L}^T$ , where  $\mathbf{L}$  is some real matrix polynomial (i.e.,  $\mathbf{L} \in \mathbb{R}[\mathbf{x}]^{n \times a}$  for some  $a$ ). For the unit norm constraints,

$$-\nabla^2 g_j = \begin{bmatrix} \sqrt{2} & 0 & 0 & 0 \\ 0 & \sqrt{2} & 0 & 0 \\ 0 & 0 & \sqrt{2} & 0 \\ 0 & 0 & 0 & \sqrt{2} \end{bmatrix} \begin{bmatrix} \sqrt{2} & 0 & 0 & 0 \\ 0 & \sqrt{2} & 0 & 0 \\ 0 & 0 & \sqrt{2} & 0 \\ 0 & 0 & 0 & \sqrt{2} \end{bmatrix}^T. \quad (22)$$

For our quaternionic loss function  $f$ , Equation 13 tells us that

$$\nabla^2 f_{i,j} = [\mathbf{Q}_{i,j} - \mathbf{I}]^T [\mathbf{Q}_{i,j} - \mathbf{I}], \quad (23)$$

which is clearly also of the form  $\mathbf{L}\mathbf{L}^T$ . Following [18], we introduce the following lemma from [1] that will help us prove  $f$  is SOS-convex.

**Lemma 1.** *A polynomial  $f \in \mathbb{R}[\mathbf{x}]$  is SOS-convex if and only if the polynomial  $\mathbf{z}^T \nabla^2 f \mathbf{z}$  is a sum of squares in  $\mathbb{R}[\mathbf{x}; \mathbf{z}]$ .*

Since each  $f_{i,j}$  is SOS-convex, Lemma 1 tells us that each term

$$\mathbf{z}^T \nabla^2 f_{i,j} \mathbf{z} \quad (24)$$

is a sum of squares. The additivity of Hessians for a sum of functions thus implies that

$$\mathbf{z}^T \nabla^2 f \mathbf{z} = \sum_{i,j} \mathbf{z}^T \nabla^2 f_{i,j} \mathbf{z} \quad (25)$$

is a sum of squares, and we can invoke the other direction of the implication in Lemma 1 to conclude that  $f$  is SOS-convex. All that remains is to show that the constraints involving the variables in block  $I_l$  (plus the polynomial 1)

generate the ring of polynomials in those variables. This requirement is easily satisfied by introducing redundant constraints of the form

$$0 \leq \frac{1}{2}(1 \pm q_{x,i}) \leq 1, \quad (26)$$

which is possible because all unit quaternion elements have magnitude less than or equal to 1. This fact is noted for the more general case of any compact semialgebraic set  $\mathbf{K}$  in Section 2.2 of [16].  $\square$

### 3.4. Chordal Cost Minimization

We are also curious as to whether the MLE/chordal formulation in Problem 7 has SOS-convex cost  $f$  and constraints  $-g_j$ . To this end, we demonstrate that orthogonality and ‘‘handedness’’ constraints defining the rotation matrix representation of elements  $\text{SO}(3)$  are *not* SOS-convex.

Let us write our rotation matrix variable as

$$\mathbf{R} = \begin{bmatrix} r_{11} & r_{12} & r_{13} \\ r_{21} & r_{22} & r_{23} \\ r_{31} & r_{32} & r_{33} \end{bmatrix} = [\mathbf{c}_1 \quad \mathbf{c}_2 \quad \mathbf{c}_3]. \quad (27)$$

The orthogonality constraints for  $\text{SO}(3)$  can be written as  $\mathbf{R}^T \mathbf{R} = \mathbf{I}$ . Expanding the constraint requiring orthogonality of columns  $\mathbf{c}_1$  and  $\mathbf{c}_2$  gives

$$g_{1,2}(\mathbf{R}) = \mathbf{c}_1^t \mathbf{c}_2 = r_{11}r_{12} + r_{21}r_{22} + r_{31}r_{32} = 0, \quad (28)$$

which has Hessian

$$\nabla^2 g_{1,2} = \begin{bmatrix} \mathbf{0}_{3 \times 3} & \mathbf{I}_{3 \times 3} & \mathbf{0}_{3 \times 3} \\ \mathbf{I}_{3 \times 3} & \mathbf{0}_{3 \times 3} & \mathbf{0}_{3 \times 3} \\ \mathbf{0}_{3 \times 3} & \mathbf{0}_{3 \times 3} & \mathbf{0}_{3 \times 3} \end{bmatrix}. \quad (29)$$

Applying Lemma 1, we obtain

$$\mathbf{z}^T \nabla^2 g_{1,2} \mathbf{z} = 2z_1z_4 + 2z_2z_5 + 2z_3z_6, \quad (30)$$

which cannot be written as a sum of squares by inspection. One might be tempted to circumvent the explicit inclusion of the column or row orthogonality constraints and define  $\text{SO}(3)$  with the following set of constraints:

$$\begin{aligned} \mathbf{c}_i^T \mathbf{c}_i &= 1, \quad i = 1, 2, 3, \\ \mathbf{c}_i^\times \mathbf{c}_j &= \mathbf{c}_k, \quad i, j, k = \text{cyclic}(1, 2, 3), \end{aligned}$$

where  $\text{cyclic}(\cdot)$  gives the cyclic permutations (including identity) of its input ordered set. However, applying the same procedure to the first element of the vector right-handedness constraint

$$\mathbf{g}_{1,2,3} = \mathbf{c}_1^\times \mathbf{c}_2 - \mathbf{c}_3 = 0 \quad (31)$$

gives us

$$\mathbf{z}^T \nabla^2 g_{1,2,3}^1 \mathbf{z} = 2z_2z_6 - 2z_3z_5, \quad (32)$$

which is once again not a sum of squares by inspection.

Since rotation matrices cannot provide the conditions (SOS-convexity of constraints) required by Sparse-BSOS for guaranteed convergence, we now consider using quaternions to represent our variables but still using the MLE cost function in Equation 8 by writing our rotation elements in the cost in terms of the following quaternion formula:

$$\mathbf{R}_i(\mathbf{q}_i) = \begin{bmatrix} 1 - 2q_y^2 - 2q_z^2 & 2q_xq_y - 2q_zq_w & 2q_xq_z + 2q_yq_w \\ 2q_xq_y + 2q_zq_w & 1 - 2q_x^2 - 2q_z^2 & 2q_yq_z - 2q_xq_w \\ 2q_xq_z - 2q_yq_w & 2q_yq_z + 2q_xq_w & 1 - q_x^2 - q_y^2 \end{bmatrix}. \quad (33)$$

Lemma 1 was employed to set up the most basic SOS feasibility program in Matlab: determining whether a polynomial is a sum of squares. The SOSTools [21] toolbox was used to solve this feasibility problem for specific values of  $\mathbf{R}_{ij}$ . In all simulated cases, which included random rotation matrices and hand picked cases like the identity matrix, SOSTools' `findsos` routine concluded that the polynomial was not a sum of squares, therefore certifying that the quartic cost in Equation 8 is not, in general, SOS-convex when using quaternion states. Thus, the theoretical global optimality guarantees are absent for the chordal formulation in Problem 7, and the algorithm we develop in Section 4 uses the quaternionic formulation in Problem 17.

## 4. Algorithm

In this section, we describe our complete approach to solving rotation averaging. This involves “pre-conditioning” the quaternion representation of measurements to mitigate the effects of the double cover property, providing a partition of the variables that satisfies the RIP, and finally using the Sparse-BSOS solver on particular problem instances.

### 4.1. Quaternion Double Cover

In Section 2, we noted the inherent problem description ambiguity caused by the double cover property of the quaternion representation of  $\text{SO}(3)$ . Since the Sparse-BSOS method requires a purely polynomial cost function, a fixed sign for each quaternion measurement  $\tilde{\mathbf{q}}_{i,j}$  must be selected. To this end, we used the method described in Section of [11] which is summarized in Algorithm 1. Although we are unaware of any formal proof demonstrating that this method always leads to an optimal assignment, the method's runtime is linear in  $M$  and  $N$  and can be empirically shown to return the optimal assignment for small ( $N \leq 10$ ) problem instances, even when severe angular measurement errors (e.g., exceeding  $\pi/2$  rad) are present.

---

### Algorithm 1 Quaternion Sign Selection [11]

---

**Input:** Edge graph  $\mathcal{E}$ , quaternion measurements  $\tilde{\mathbf{q}}_{i,j}$

**Output:** Quaternion signs  $\epsilon_{i,j} \in \{-1, 1\}$ ,  $\forall (i, j) \in \mathcal{E}$

```

1: function QUATERNIONSIGNS( $\mathcal{E}$ ,  $\tilde{\mathbf{q}}_{i,j}$ )
2:    $\mathcal{T} \leftarrow \text{SpanningTree}(\mathcal{E}) \triangleright$  Form a spanning tree of  $\mathcal{E}$ 
3:    $\mathbf{q}_1 \leftarrow [1; 0; 0; 0] \triangleright$  Set root vertex to identity
4:   for  $(i, j) \in \mathcal{T}$  do
5:      $\mathbf{q}_j \leftarrow \mathbf{q}_i \circ \tilde{\mathbf{q}}_{i,j}$ 
6:      $\epsilon_{i,j} \leftarrow 1$ 
7:   for  $(i, j) \in \mathcal{E} \setminus \mathcal{T}$  do
8:      $\epsilon_{i,j} \leftarrow \underset{\epsilon \in \{-1, 1\}}{\text{argmin}} \mathbf{q}_i \circ \epsilon \tilde{\mathbf{q}}_{i,j}$ 
9:   return  $\{\epsilon_{i,j}\}_{(i,j) \in \mathcal{E}}$ 

```

---

### 4.2. The Running Intersection Property

The RIP holds if there exists  $p \in \mathbb{N}$  and subsets  $I_l \subseteq [N]$  and  $J_l \subseteq [M]$  for all  $l \in [p]$  such that:

- $f = \sum_{l=1}^p f^l$ , for some  $f^1, \dots, f^p$  such that  $f^l \in \mathbb{R}[\mathbf{x}; I_l]$ ,  $l \in [p]$ ;
- $g_j \in \mathbb{R}[\mathbf{x}; I_l]$  for all  $j \in J_l$  and  $l \in \{1, \dots, p\}$ ;
- $\bigcup_{l=1}^p I_l = [N]$ ;
- $\bigcup_{l=1}^p J_l = [M]$ ;
- for all  $l \in [p-1]$  there exists  $s \leq l$  such that  $(I_{l+1} \cap \bigcup_{r=1}^l I_r) \subseteq I_s$ .

Note that the simple partitioning  $p = 1$ ,  $I_1 = \{1, \dots, N\}$  trivially satisfies the RIP but does not retain the sparsity pattern that makes the Sparse-BSOS solution method faster than non-sparse alternatives. The problem of finding the “optimal” (i.e., in some sense *sparsest*) partitioning that satisfies the RIP is a challenging problem. Like the approach in [18], we use the fast but suboptimal junction tree-construction method of [23] to produce partitions that satisfy the RIP. This method requires a sequence  $(C_1, \dots, C_k)$  of  $I = \{1, \dots, N\}$  which covers  $I$  (i.e.,  $\bigcup_{i=1}^k C_i = I$ ) as input. In order for the first requirement above (i.e., all variables involved in monomial  $f^l$  can be found in the partition  $I_l$ ) to hold, we use the edges  $\mathcal{E}$  as our covering sequence. This quick and simple choice may affect the quality of the resulting partition, but we leave characterizing the effect of the variable partition on performance for future work. Algorithm 2 summarizes the method used at a high level; please see our open source implementation in Matlab for further details.

### 4.3. Sparse-BSOS Rotation Averaging

Our complete Sparse-BSOS Rotation Averaging method is presented in Algorithm 3. It takes as input a specification

---

**Algorithm 2** Satisfy RIP via Junction Tree Algorithm [23]

**Input:** Variable edge graph  $\mathcal{E}$ , variable partition  $\{I_l\}_{l=1}^p$   
**Output:** Variable/constraint partitions  $\{I_l, J_l\}_{l=1}^p$  satisfying RIP

- 1: **function** SATISFYRIP( $\mathcal{E}$ )
- 2:  $(C_1, \dots, C_m) \leftarrow \text{SortByMinVertex}(\mathcal{E})$
- 3:  $(Q_1, \dots, Q_{r'}) \leftarrow \text{Merge}((C_1, \dots, C_m) \triangleright \text{Form unions with } C_i \text{ that share their smallest element})$
- 4:  $(Q_1, \dots, Q_r) \leftarrow \text{MakeProperSequence}((Q_1, \dots, Q_{r'}))$   
 $\triangleright \text{Clean the sequence by removing any subsets of other sets}$
- 5:  $(C_1, \dots, C_k) \leftarrow \text{JunctionTree}((Q_1, \dots, Q_r))$
- 6:  $\{I_l\}_{l=1}^p \leftarrow \text{MakeProperSequence}((C_1, \dots, C_k))$
- 7:  $\{J_l\}_{l=1}^p \leftarrow \text{MapToConstraints}(\{I_l\}_{l=1}^p)$
- 8: **return**  $\{I_l\}_{l=1}^p, \{J_l\}_{l=1}^p$

---

of Problem 11 in the form of an edge graph  $\mathcal{E}$  and corresponding noisy measurements  $\tilde{\mathbf{q}}_{i,j}$ . The measurement signs  $\epsilon_{i,j}$  are selected with Algorithm 1 and applied to  $\tilde{\mathbf{q}}_{i,j}$ . Next, a variable partition  $\{I_l\}_{l=1}^p$  covering  $[N]$  that satisfies the RIP described in Section 4.2 is found with Algorithm 2. Finally, the SOS-convex polynomial program in Problem 17 is instantiated and solved with the Sparse-BSOS software package of [27].

---

**Algorithm 3** Sparse-BSOS Rotation Averaging

**Input:** Variable edge graph  $\mathcal{E}$ , quaternion measurements  $\tilde{\mathbf{q}}_{i,j}$   
**Output:** Globally optimal solution  $\{\mathbf{q}_i^*\}_{i=1}^N$

- 1: **function** JUNCTIONTREE( $\mathcal{E}, \{I_l\}_{l=1}^p$ )
- 2:  $\{\epsilon_{i,j}\}_{(i,j) \in \mathcal{E}} \leftarrow \text{QuaternionSigns}(\mathcal{E}, \tilde{\mathbf{q}}_{i,j})$
- 3: **for**  $(i, j) \in \mathcal{E}$  **do**
- 4:  $\tilde{\mathbf{q}}_{i,j} \leftarrow \epsilon_{i,j} \tilde{\mathbf{q}}_{i,j}$
- 5:  $\{I_l\}_{l=1}^p, \{J_l\}_{l=1}^p \leftarrow \text{SatisfyRIP}(\mathcal{E})$
- 6:  $\{\mathbf{q}_i^*\}_{i=1}^N \leftarrow \text{Sparse-BSOS}(\mathcal{E}, \tilde{\mathbf{q}}_{i,j}, \{I_l, J_l\}_{l=1}^p)$
- 7: **return**  $\{\mathbf{q}_i^*\}_{i=1}^N$

---

## 5. Experiments

In this section, we provide results on experiments using synthetic data (see the supplementary material for more extensive results). We use multiple simulated problem instances with perfect ground truth to demonstrate that the theoretical guarantee of global optimality is borne out in practice, and to demonstrate the advantages of our approach. For each random problem instance,  $N$  rotation matrices indexed from  $1, \dots, N$  are uniformly sampled and edges connecting connecting rotations  $i$  and  $i + 1$  are added to the edge graph  $\mathcal{E}$ . Then,  $n_l$  ‘loop closures’ between non-

consecutive rotations are introduced by randomly sampling pairs without replacement. The notion of a loop closure is used in robotics to indicate when a robot has returned to a location it previously observed. Thus, each randomly generated rotation averaging problem instance has  $N - 1 + n_l$  edges representing pairwise measurements.

In all experiments, error is introduced to idealized ground truth rotation matrix measurements via an axis-angle perturbation where the axis is uniformly sampled over the unit sphere, and the magnitude of rotation is drawn from a uniform distribution over  $[-\theta_{\max}, \theta_{\max}]$ . This noise injection strategy was chosen because unlike the chordal loss of 8, the quaternionic loss is not a MLE estimate. Additionally, the uniform distribution, unlike a Gaussian or von Mises distribution, provides a hard bound on the maximum single measurement error present in a problem instance. In all cases presented, semidefinite programs (SDPs) are solved by the SDPT3 Matlab software [25]. This is a popular, generic SDP solver that is not specifically tailored to problems exhibiting any specific structure (see Section 5.3 for further discussion).

### 5.1. Global Optimality

In every single simulated problem instance, our approach (Algorithm 3) produced a certifiably global minimum. Curiously, the Lagrangian duality-based approach of Fredriksson et al. in [9] also returned the global minimum in all tested instances, even though we are unaware of a proof of its optimality. Please see the supplementary material for detailed results and further discussion.

### 5.2. Error Analysis

To investigate the accuracy benefits of a globally optimal approach, we use the following mean quaternion norm error between an estimate  $\{\mathbf{q}_i^*\}_{i=1}^N$  and the ground truth  $\{\mathbf{q}_i\}_{i=1}^N$ :

$$\frac{1}{N} \sum_{i=1}^N \min(\|\mathbf{q}_i - \mathbf{q}_i^*\|_2, \|\mathbf{q}_i + \mathbf{q}_i^*\|_2). \quad (34)$$

Figure 2 compares the performance in terms of this metric for our approach (labelled ‘SBSOS’) and a common local optimization method (labelled ‘Local’). In the local approach, the measurements corresponding to sequential edges  $i, i + 1$ , along with the fixed initial pose value  $\mathbf{q}_0$  are used to initialize the values of each  $\mathbf{q}_i$ . Then, Matlab’s local `fmincon` function is used to locally optimize the cost function. Our globally optimal approach has markedly better accuracy when the maximum angular error  $\theta_{\max} \leq 0.5\pi$  rad. Additionally, increasing the graph density (via  $n_l$ ) also improves the relative performance of SBSOS over Local.

### 5.3. Runtime

In this section, we compare the runtime of our algorithm and the SDP relaxation of Fredriksson et al. found in [9].

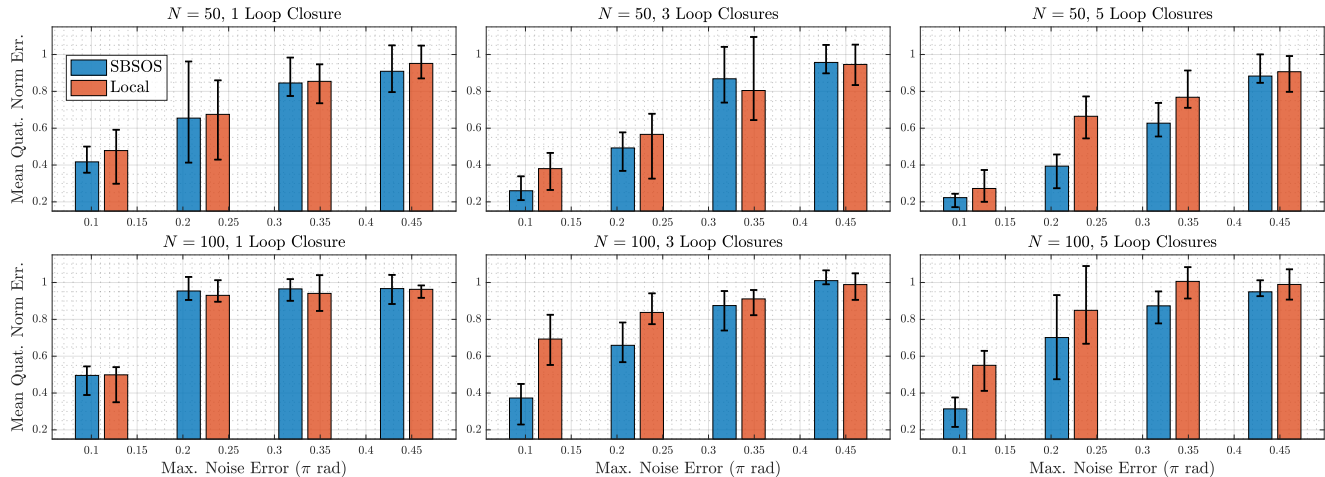


Figure 2: Mean quaternion norm error for SBSOS and Local methods. Each bar chart specifies a value of  $N$  and  $n_l$ , while each individual bar represents the mean over 10 random runs for a value of  $\theta_{\max}$ , which varies along the x-axis. The error bars represent the 1st and 3rd quartile over the 10 random runs.

Figure 3 compares the mean runtime of each approach over 10 runs for a variety of  $N$  and  $n_l$  values. For the parameter range displayed, it is clear that our approach exploits sparsity to run faster than the standard SDP relaxation (labelled ‘Fredriksson’), which scales very poorly with  $N$ . However, for values of  $n_l$  greater than 5, the mean and variance of the SBSOS runtime begins to increase rapidly, often taking much longer than the standard SDP. Further investigation into choosing a partition over dense edge graphs is needed to ensure a reasonable runtime. However, large sparse graphs are common in robotics applications where a vehicle navigating a large environment infrequently returns to previously visited areas. The runtime of local methods like the one described in Section 5.2 is much faster (e.g., less than a second for over a hundred poses in Matlab) than our certifiably globally optimal approach, which does not scale well with graph density. However, there is great promise that fast block-coordinate minimization (BCM) algorithms like the one used for chordal rotation averaging in [8] can be applied to our approach and Fredriksson et al.’s SDP relaxation. Recent work has provided formal guarantees that these methods can find the global minimum to SDPs formed by relaxing problems involving unit norm and orthogonality constraints in a fraction of the time taken by interior-point methods like SDPT3 [24, 7]. In this paper’s sequel, we intend to apply these methods (and their associated theoretical machinery) to both the standard SDP relaxation and the SDP resulting from our application of the Sparse-BSOS hierarchy to rotation averaging.

## 6. Conclusion and Future Work

In this paper, we have presented the first application of sum of squares optimization techniques to 3D rotation aver-

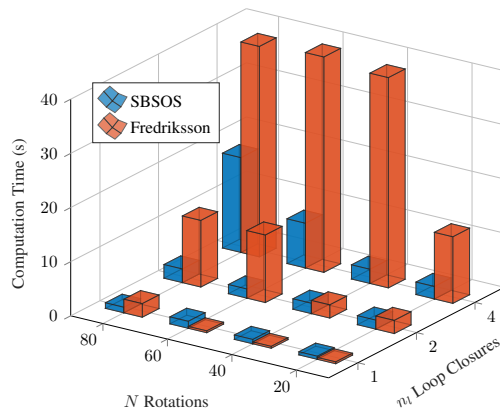


Figure 3: Comparison of solver runtimes for Fredriksson’s SDP relaxation [9] and SBSOS for  $\theta_{\max} = \frac{2\pi}{10}$ . Each bar displays the mean runtime in seconds over 10 runs.

aging, resulting in the first algorithm that is *guaranteed* to find a global minimum of *any* problem instance. We leveraged the approach for 2D SLAM in [18] to provide proofs of finite convergence of Sparse-BSOS on a quaternionic loss function. This is an important step towards fast and provably optimal methods for solving rotation averaging, which forms the backbone of many SfM algorithms and other related tasks in computer vision and robotics.

In addition to further experimentation on real and synthetic data, a thorough investigation into block-coordinate minimization methods for convex relaxations of rotation averaging will lead to faster runtimes [24, 7]. Finally, a comparison with other rotation averaging schemes and cost functions is needed, especially those that have similar optimality guarantees [8].



## References

- [1] A. A. Ahmadi and P. A. Parrilo. Sum of squares and polynomial convexity. In *Proc. IEEE Control and Decision Conference*, 2009. 5
- [2] J. Briales and J. Gonzalez-Jimenez. Cartan-sync: Fast and global se (d)-synchronization. *IEEE Robotics and Automation Letters*, 2(4):2127–2134, 2017. 1, 2
- [3] J. Briales, L. Kneip, S. ShanghaiTech, and J. Gonzalez-Jimenez. A certifiably globally optimal solution to the non-minimal relative pose problem. In *Proceedings of the IEEE Conference on Computer Vision and Pattern Recognition*, pages 145–154, 2018. 2
- [4] C. Cadena, L. Carlone, H. Carrillo, Y. Latif, D. Scaramuzza, J. Neira, I. Reid, and J. J. Leonard. Past, present, and future of simultaneous localization and mapping: Toward the robust-perception age. *IEEE Transactions on Robotics*, 32(6):1309–1332, 2016. 1
- [5] L. Carlone, D. M. Rosen, G. Calafiore, J. J. Leonard, and F. Dellaert. Lagrangian duality in 3d slam: Verification techniques and optimal solutions. In *Intelligent Robots and Systems (IROS), 2015 IEEE/RSJ International Conference on*, pages 125–132. IEEE, 2015. 2, 3
- [6] L. Carlone, R. Tron, K. Daniilidis, and F. Dellaert. Initialization techniques for 3d slam: a survey on rotation estimation and its use in pose graph optimization. In *Robotics and Automation (ICRA), 2015 IEEE International Conference on*, pages 4597–4604. IEEE, 2015. 1
- [7] M. A. Erdogdu, A. Ozdaglar, P. A. Parrilo, and N. D. Vanli. Convergence rate of block-coordinate maximization burer-monteiro method for solving large sdps. *arXiv preprint arXiv:1807.04428*, 2018. 8
- [8] A. Eriksson, C. Olsson, F. Kahl, and T.-J. Chin. Rotation averaging and strong duality. In *Proceedings of the IEEE Conference on Computer Vision and Pattern Recognition*, pages 127–135, 2018. 1, 2, 8
- [9] J. Fredriksson and C. Olsson. Simultaneous multiple rotation averaging using lagrangian duality. In *Asian Conference on Computer Vision*, pages 245–258. Springer, 2012. 2, 7, 8
- [10] M. Giamou, Z. Ma, V. Peretroukhin, and J. Kelly. Certifiably globally optimal extrinsic calibration from per-sensor ego-motion. *IEEE Robotics and Automation Letters*, 4(2):367–374, 2019. 2
- [11] R. Hartley, J. Trunpf, Y. Dai, and H. Li. Rotation averaging. *International journal of computer vision*, 103(3):267–305, 2013. 1, 3, 6
- [12] J. Heller, D. Henrion, and T. Pajdla. Hand-eye and robot-world calibration by global polynomial optimization. In *Robotics and Automation (ICRA), 2014 IEEE International Conference on*, pages 3157–3164. IEEE, 2014. 2
- [13] F. Ke, J. Xie, Y. Chen, and D. Zhang. Global rotation estimation for stereo camera systems. *Optik*, 126(23):4022–4025, 2015. 2
- [14] J. B. Lasserre. Global optimization with polynomials and the problem of moments. *SIAM Journal on optimization*, 11(3):796–817, 2001. 2
- [15] J.-B. Lasserre. *Moments, positive polynomials and their applications*, volume 1. World Scientific, 2010. 2, 4
- [16] J. B. Lasserre. A lagrangian relaxation view of linear and semidefinite hierarchies. *SIAM Journal on Optimization*, 23(3):1742–1756, 2013. 5
- [17] J. B. Lasserre, K.-C. Toh, and S. Yang. A bounded degree sos hierarchy for polynomial optimization. *EURO Journal on Computational Optimization*, 5(1-2):87–117, 2017. 4
- [18] J. G. Mangelson, J. Liu, R. M. Eustice, and R. Vasudevan. Guaranteed globally optimal planar pose graph and landmark slam via sparse-bounded sums-of-squares programming. *arXiv preprint arXiv:1809.07744*, 2018. 1, 2, 4, 5, 6, 8
- [19] C. Olsson and A. Eriksson. Solving quadratically constrained geometrical problems using lagrangian duality. In *Pattern Recognition, 2008. ICPR 2008. 19th International Conference on*, pages 1–5. IEEE, 2008. 2
- [20] P. A. Parrilo. Semidefinite programming relaxations for semialgebraic problems. *Mathematical programming*, 96(2):293–320, 2003. 2, 4
- [21] S. Prajna, A. Papachristodoulou, and P. A. Parrilo. Introducing sostools: A general purpose sum of squares programming solver. In *Decision and Control, 2002, Proceedings of the 41st IEEE Conference on*, volume 1, pages 741–746. IEEE, 2002. 6
- [22] D. M. Rosen, L. Carlone, A. S. Bandeira, and J. J. Leonard. Se-sync: A certifiably correct algorithm for synchronization over the special euclidean group. *arXiv preprint arXiv:1612.07386*, 2016. 1, 2
- [23] L. Smail. Junction trees constructions in bayesian networks. In *Journal of Physics: Conference Series*, volume 893, page 012056. IOP Publishing, 2017. 6, 7
- [24] Y. Tian, K. Khosoussi, and J. P. How. Block-coordinate minimization for large sdps with block-diagonal constraints. *arXiv preprint arXiv:1903.00597*, 2019. 8
- [25] K.-C. Toh, M. J. Todd, and R. H. Tütüncü. Sdpt3a matlab software package for semidefinite programming, version 1.3. *Optimization methods and software*, 11(1-4):545–581, 1999. 7
- [26] L. Wang and A. Singer. Exact and stable recovery of rotations for robust synchronization. *Information and Inference: A Journal of the IMA*, 2(2):145–193, 2013. 1, 2
- [27] T. Weisser, J. B. Lasserre, and K.-C. Toh. Sparse-bsos: a bounded degree sos hierarchy for large scale polynomial optimization with sparsity. *Mathematical Programming Computation*, 10(1):1–32, 2018. 2, 4, 5, 7
- [28] K. Wilson, D. Bindel, and N. Snavely. When is rotations averaging hard? In *European Conference on Computer Vision*, pages 255–270. Springer, 2016. 2

# Supplementary Material for “Sparse Bounded Degree Sum of Squares Optimization for Certifiably Globally Optimal Rotation Averaging”

Matthew Giamou\*, Filip Maric, Valentin Peretroukhin, Jonathan Kelly  
University of Toronto

## 1. Introduction

This supplementary material contains some figures and comments summarizing experimental results that were unable to fit in the main body of the paper “Sparse Bounded Degree Sum of Squares Optimization for Certifiably Globally Optimal Rotation Averaging”. Specifically, more data on algorithm runtimes and global optimality are provided.

## 2. Runtime

In addition to the lower noise ( $\theta_{\max} = 2\pi/10$ ) case in Figure 3 of the main paper, we present the noisier  $\theta_{\max} = 9\pi/10$  case in Figure 1. Once again, SBSOS scales much better with respect to the number of variables  $N$  than the standard SDP relaxation of Fredriksson et al., but struggles with increasing graph density (i.e., when the number of loop closures  $n_l$  is large). However, the trend of increasing SBSOS runtime for increasing  $n_l$  is a bit less severe in the noisier case of Figure 1. We do not have an explanation for this behaviour at the moment but intend to investigate this phenomenon in future work.

## 3. Global Optimality

In the main paper, we mentioned that the Sparse-BSOS method and SDP relaxation both returned the same certifiably globally optimal minimum for all test cases. In this section, we compare the cost function of the local method with the globally optimal cost function value. Figure 2 displays the mean objective function values for the same set of random runs displayed in Figure 2 of the main paper. As predicted by the theory dictating that SBSOS will always return the global minimum, the local method is worse in every single case. This verifies the hypothesis that the worse error results at low noise displayed in Figure 2 of the main paper are due to the local method becoming trapped in local minima. At higher noise levels, the globally optimal method still finds much better solutions in terms of the objective function, but this is not strongly reflected in

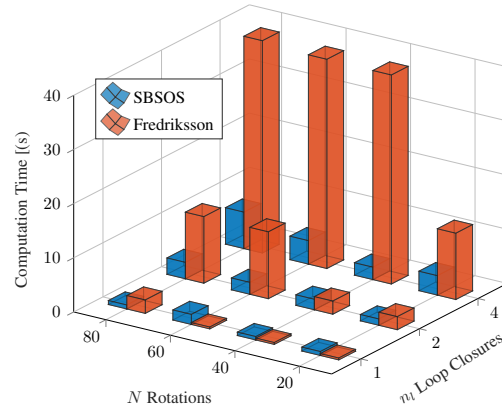


Figure 1: Comparison of solver runtimes for Fredriksson et al.’s SDP relaxation [1] and our SBSOS method for  $\theta_{\max} = \frac{9\pi}{10}$ . Each bar displays the mean runtime in seconds over 10 runs.

the actual error as the severe noise erodes the value of the true global minimum. The experiments in [1] provide a use case for global optimality in high-error problem instances in the context of an iterative-reweighted least squares (IRLS) solver for robust cost functions. Robust cost functions mitigate the effects of outliers which contain arbitrarily high measurement error on optimization problems. The IRLS method approximates robust cost functions with a sequence of weighted least squares problems that are easier to solve. We intend to investigate these methods and attempt to characterize cases where global optimality aids in providing an accurate estimate.

## References

- [1] J. Fredriksson and C. Olsson. Simultaneous multiple rotation averaging using lagrangian duality. In *Asian Conference on Computer Vision*, pages 245–258. Springer, 2012. 1

\*The corresponding author can be reached at matthew.giamou@robotics.utias.utoronto.ca.

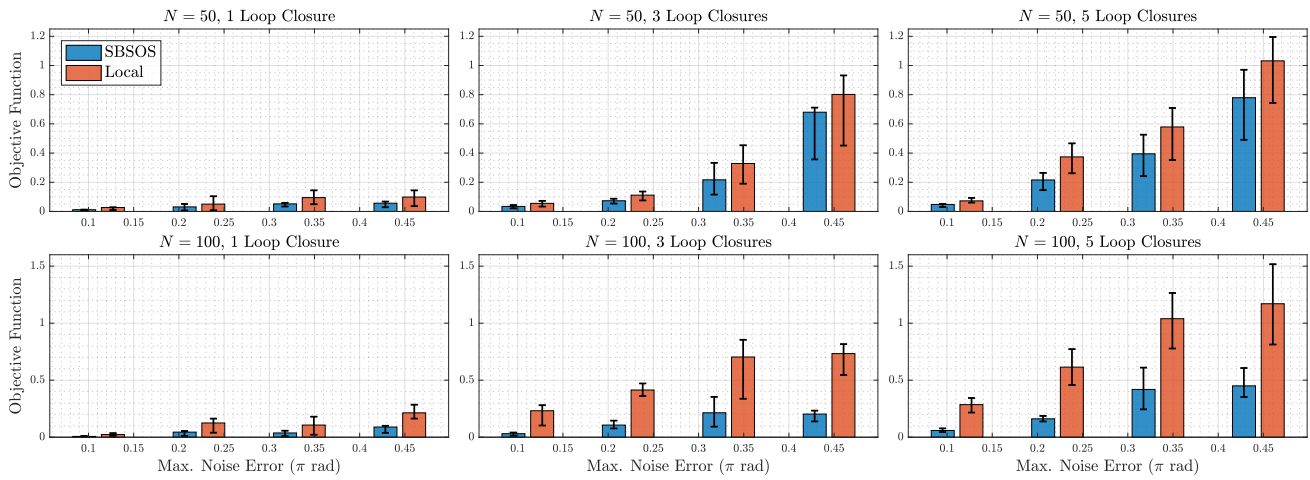


Figure 2: Mean objective function values for SBSOS and Local methods. Each bar chart specifies a value of  $N$  and  $n_l$ , while each individual bar represents the mean value of the objective function over 10 random runs for a value of  $\theta_{\max}$ , which varies along the x-axis. The error bars represent the 1st and 3rd quartile over the 10 random runs. The values returned by SBSOS were certified as globally optimal via the absence of an objective function gap between the original and relaxed problems, whereas the local method is clearly returning solutions corresponding to local minima.